Catal Lett (2008) 124:384–391
DOI 10.1007/s10562-008-9481-x

Effect of P Content on the Catalytic Performance of P-modified HZSM-5 Catalysts in Dehydration of Ethanol to Ethylene

Dongsheng Zhang · Rijie Wang · Xiaoxia Yang

Received: 20 December 2007 / Accepted: 21 March 2008 / Published online: 8 April 2008

Abstract A series of phosphorus (P) modified HZSM-5 catalysts were prepared and characterized with various techniques. These catalysts were used in dehydration of ethanol to ethylene at different temperatures. It was found that not all the P-modified catalysts favor this reaction at high temperatures. Over the catalyst with 3.4 wt% P, the main product is ethylene at 573–713 K, due to the presence of weak acid sites after P modification. When the P loading is below 3.4 wt%, ethylene and higher hydrocarbons are observed at high temperatures. As P content is above 3.4 wt%, higher reaction temperature is necessary for ethanol dehydration to ethylene.

Keywords Phosphorous · HZSM-5 · Dehydration · Ethanol · Ethylene

1 Introduction

Ethylene is an essential raw material for the petrochemical industry, which is mainly derived from natural gas or petroleum. However, in view of the energy crisis, the production of ethylene from ethanol has received widespread attention in recent years [1–5], as ethanol can be obtained easily from renewable biomass by fermentation.

Many researchers have investigated catalytic dehydration of ethanol to ethylene over HZSM-5 zeolite [6–11]. These studies revealed that low temperature (543–593 K) favors the reaction of ethanol dehydration, and high temperature (623–723 K) hinders this reaction. At high reaction temperatures, higher hydrocarbons (C_3–C_{9+} aliphatic and aromatic) occurred to a significant extent [12, 13]. However, when the HZSM-5 was modified with zinc or manganese [14], alkaline-earth metals and lanthanides [15], magnesium and copper [16], the yield of ethylene was enhanced greatly. Recently, Tynjälä et al. [17] found that ethylene was the final product over phosphorus (P) modified HZSM-5 catalysts containing 2.2 and 2.7 wt% P (correspond to P/Al atomic ratios of around 1.9 and 2.8, respectively). No further conversion of ethylene to higher hydrocarbons was observed at high reaction temperature (643 K). Then arises a question. Do the P-modified HZSM-5 samples with different amounts of P (especially P/Al < 1.9) have the same effect? To answer this question, we investigated the dehydration of ethanol at different temperatures over P-modified HZSM-5 with various contents of P. To the best of our knowledge, this is still seldom reported so far.

2 Experimental

2.1 Catalyst Preparation

HZSM-5 zeolite ($SiO_2/Al_2O_3 = 25$) was supplied by Nankai University, China. The P-modified HZSM-5 samples were prepared by impregnating the HZSM-5 zeolite with aqueous solution containing desired amount of phosphoric acid, followed by drying at room temperature for 12 h and 383 K for 2 h, and finally calcinations at 823 K for 3 h. The samples were pelleted, crushed and then sieved to 20–30 mesh for catalytic testing and characterization. The P contents were 1.9, 3.2, 3.4, 3.6 and 5.1 wt%, which correspond to P/Al atomic ratios of 0.5, 0.9, 0.95, 1.0 and 1.5 respectively. P-modified HZSM-5 samples containing x wt% P were denoted as PZ-x.

D. Zhang · R. Wang · X. Yang (✉)
School of Chemical Engineering and Technology, Tianjin University, Tianjin 300072, People's Republic of China
e-mail: xxytju@yahoo.cn

2.2 Characterization

Phase identification was performed by X-ray diffraction (XRD) using a PANalytical X'Pert Pro computerized diffractometer with Co Kα radiation operated at 40 kV and 30 mA. The 2θ value was scanned in the range of 5–80°. The relative crystallinity of the ZSM-5 samples was calculated from the peak area of $2\theta = 26$–$30°$ in the XRD spectra, using the HZSM-5 sample as reference.

The chemical composition of the catalysts was determined by X-ray fluorescence (XRF) using a SHIMADZU XRF-1800 spectrometer.

Surface area, pore volume and pore diameter of the samples were measured by nitrogen adsorption–desorption at 77 K using a Quantachrome Autosorb-1 instrument. The pore volume and pore diameter were estimated from the Horvath-Kawazoe (HK) method, and the surface area was calculated by Brunauer–Emmett–Teller (BET) method.

Nuclear magnetic resonance (NMR) experiments were performed on a Varian InfinityPlus300 NMR spectrometer equipped with a magic angle of spinning (MAS) probe. ^{27}Al NMR spectra were recorded at 78.13 MHz with a spinning rate of 10.0 kHz, a pulse width of 0.6 μs and a pulse delay of 3.0 s. The ^{27}Al chemical shifts were referenced externally to an aqueous solution of $Al(NO_3)_3$ (0 ppm).

The temperature programmed desorption of ammonia (NH_3-TPD) measurements were carried out on a conventional setup equipped with a thermal conductivity detector. Catalyst samples (100 mg) were activated at 823 K for 1 h and then cooled to 300 K in a flow of nitrogen (35 mL/min). The adsorption of ammonia was performed at this temperature. Physically adsorbed NH_3 was removed at 373 K. And then NH_3-TPD was performed by heating the sample at a rate of 15 K/min from 373 K to 823 K. The signal was recorded by a thermal conductivity detector.

The coke content deposited in the used catalysts was determined by combustion in a thermogravimetric (TG) analyzer. The temperature was raised from 313 K to 1073 K with a ramp of 10 K/min.

2.3 Catalytic Testing

The reaction was carried out in a continuous flow fixed-bed reactor. The catalyst was put into the reactor and activated at 553 K for 1 h in a small stream of nitrogen before reaction, and the nitrogen flow (10 mL/min) was kept during reaction. Pure ethanol (≥99.9%) was introduced to a vaporizer using a micro liquid pump before passing into the reactor. Usually, the reactor was loaded with 1.5 g of catalyst, the pressure was kept at 0.1 MPa and the weight hourly space velocity (WHSV) was 3.0 h^{-1}. The reaction temperatures were raised from 553 K to 713 K. After each increment, the system was allowed to stabilize for 2 h on stream before measuring.

The reaction products were analyzed by a SP-3420 gas chromatography (on-line system) equipped with a flame ionization detector and an Agilent HP 5973 N gas chromatography-mass spectrometry (off-line system) equipped with both a flame ionization detector and a mass selective detector. A capillary column of PEG-20 M was used for most analyses. The measurements were repeated at least two times to check the reproducibility. The results did not differ by more than ±2.5% from the average values. The products were identified by the gas chromatography-mass spectrometry. The concentrations of organic components in the reactor effluent stream, expressed as weight percentages, were determined from the on-line chromatographic results. The response factors in gas chromatography analysis were evaluated from the effective carbon number method proposed by Scanlon and Willis [18, 19], expressed on a weight response basis relative to benzene. Ethanol conversion (X_{EtOH}) and products selectivity values (S_i) were calculated by the following Eqs. 1, 2:

$$X_{EtOH} = \left[1 - \frac{2\frac{W_{EtOH}}{M_{EtOH}}}{\sum\left(n_i \frac{W_i}{M_i}\right)}\right] \cdot 100\% \quad (1)$$

$$S_i = \frac{W_i}{\sum_{i \neq EtOH} W_i} \cdot 100\% \quad (2)$$

Where: W_i is the weight percentage of i component in the reactor effluent, M_i is the molar mass of i component, n_i is the number of carbon atoms in each molecule of i component.

3 Results and Discussion

3.1 Physicochemical Properties of Catalyst

The chemical composition and textural properties of parent and P-modified HZSM-5 samples are listed in Table 1. The XRD patterns of all catalysts are shown in Fig. 1. It can be seen from Fig. 1 that all the samples are typical MFI-type structure and present no additional phase. However, there is a clearly decrease in the relative crystallinity (Table 1), especially for high P contents. The reason may be the framework defects caused by dealumination [20], as demonstrated in ^{27}Al MAS NMR spectra (see Fig. 3). Figure 2 gives the pore size distributions of the samples. A slight shift of most probable pore diameter to small size is observed for the P-modified HZSM-5 catalysts, indicating the reduction of the pore dimensions. The BET analysis in Table 1 shows that the surface area (S_{BET}) of P-modified HZSM-5 decreases as the increases of P content. It is likely due to the reduction of pore dimensions or partial pore blockage of the HZSM-5 by the P species introduced in the treatment [17, 21]. This conclusion is verified by the decrease of micro pore volume in Table 1.

Table 1 Chemical composition and textural properties of parent and P-modified HZSM-5 samples

Sample	Si/Al (mol/mol)[a]	P/Al (mol/mol)[a]	XRD (%)[b]	S_{BET} (m^2/g)[c]	V_P (cm^3/g)[d]
HZSM-5	12.32	0	100	291.6	0.145
PZ-1.9	12.23	0.48	89.07	211.1	0.105
PZ-3.2	12.26	0.89	88.35	174.0	0.087
PZ-3.4	12.18	0.97	75.16	159.5	0.081
PZ-3.6	12.15	1.06	74.75	157.9	0.079
PZ-5.1	12.06	1.66	62.05	48.24	0.023

[a] Determined by XRF
[b] The relative crystallinity
[c] The BET surface area
[d] The micro pore volume

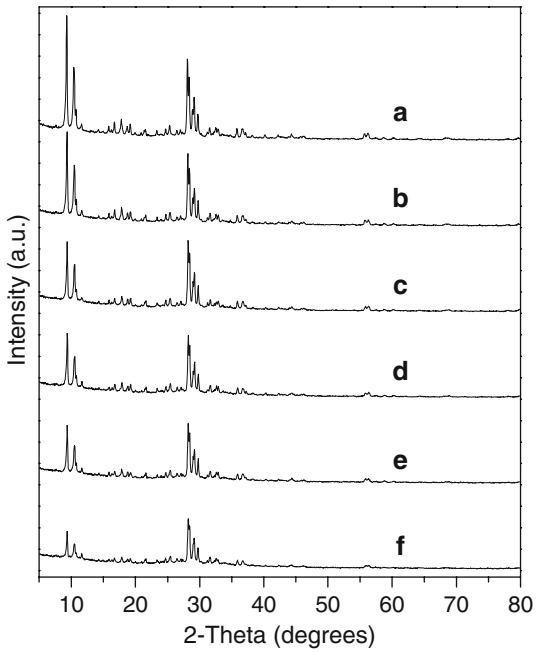

Fig. 1 XRD patterns of parent and P-modified HZSM-5: (**a**) HZSM-5; (**b**) PZ-1.9; (**c**) PZ-3.2; (**d**) PZ-3.4; (**e**) PZ-3.6; (**f**) PZ-5.1

The ^{27}Al MAS NMR spectra were used to determine the coordinations of the aluminum species present in the HZSM-5 samples. Figure 3 shows the ^{27}Al MAS NMR spectra of parent and P-modified samples. For the parent HZSM-5 sample, a relatively sharp resonance can be seen clearly at 54 ppm representing tetrahedral framework aluminum (TFAL) species, and a small resonance at around 0 ppm is observed, assigned to extra-framework aluminum (EFAL) species in octahedral or penta-coordination [22]. When the HZSM-5 catalyst was modified with certain amounts of P, a new resonance at −14 ppm appeared. As P content in the zeolite increases, the area of the resonance peak increases and the resonance moves slightly to lower chemical shift values. This may be assigned to octahedral Al species attached to P probably in the form of aluminum phosphates [23]. However, the resonance at 54 ppm becomes weaker with increasing P content. This may be a consequence of dealmination of TFAL in the HZSM-5 framework [24]. It can be deduced that the framework of the sample modified with P was changed, which is well in agreement with the results of XRD (see Table 1). In addition, a small resonance at around 38 ppm is also observed in Fig. 3c, which would be

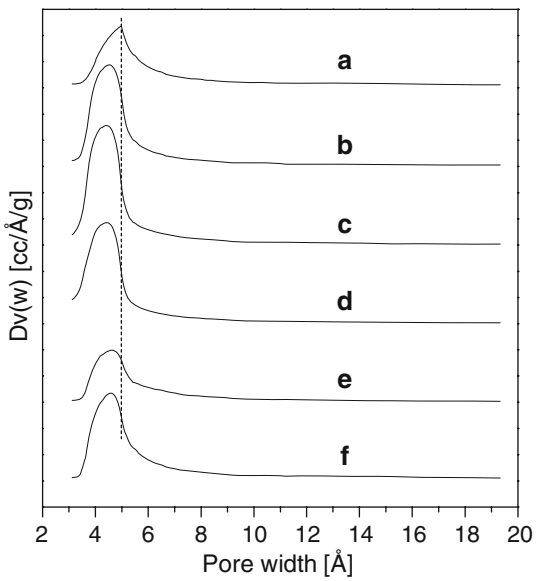

Fig. 2 Pore size distributions of parent and P-modified HZSM-5: (**a**) HZSM-5; (**b**) PZ-1.9; (**c**) PZ-3.2; (**d**) PZ-3.4; (**e**) PZ-3.6; (**f**) PZ-5.1

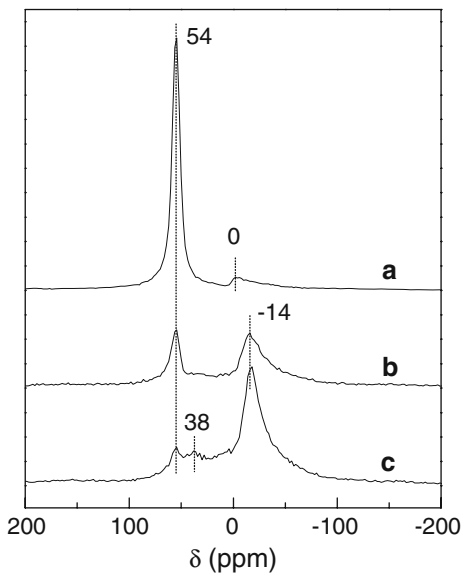

Fig. 3 ^{27}Al MAS NMR spectra of parent and P-modified HZSM-5: (**a**) HZSM-5; (**b**) PZ-3.4; and (**c**) PZ-5.1

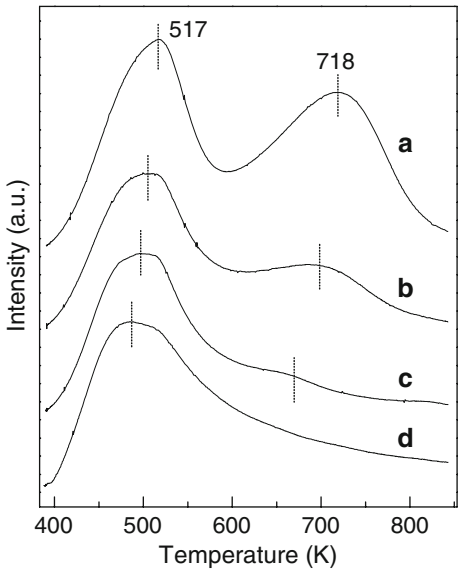

Fig. 4 NH_3-TPD profiles of parent and P-modified HZSM-5: (**a**) HZSM-5; (**b**) PZ-1.9; (**c**) PZ-3.4; (**d**) PZ-5.1

intermediate aluminum species. They can be either TFAL species in a distorted environment or EFAL species [25].

NH_3-TPD measurement was carried out to study the acidic properties of the catalysts. Figure 4 is the results of parent and P-modified HZSM-5 samples. Generally, there are two NH_3-desorption peaks for HZSM-5 zeolite. The peak at higher temperature is due to desorption of ammonia chemisorbed at strong acid sites, and that at lower temperature is assigned to weak acid sites. These two peaks located at temperatures of 517 K and 718 K can be seen clearly on HZSM-5 in Fig. 4a. After the introduction of P, the high-temperature peak shifts to low temperature and the peak area decreases significantly. Furthermore, this tendency becomes more apparent when the P loading is 3.4 wt%. For this catalyst, only one peak due to weak acid sites is observed clearly (Fig. 4c). The obtained results can be attributed to dealumination of TFAL in the HZSM-5 framework (see Fig. 3), which is primarily responsible for the strong acidity of the catalysts [26]. Moreover, the low-temperature peak also shifts slightly toward low temperatures as P content increases, indicating the replacement of the strong acid sites by new acidic centers caused by the introduction of P [27].

3.2 Effect of P Content on Catalytic Performance of the Catalyst

The product distribution over parent and P-modified HZSM-5 samples at different reaction temperatures is given in Tables 2–4. In the case of parent HZSM-5 catalyst, ethanol was completely converted to hydrocarbons under all experimental conditions. As shown in Table 2, the main product is

Table 2 Product distribution at different temperatures over HZSM-5 and PZ-1.9 catalysts

	HZSM-5						PZ-1.9					
	Temperature (K)											
	553	573	613	653	673	713	553	573	613	653	673	713
Ethanol conversion (%)	100	100	100	100	100	100	97.6	100	100	100	100	100
Selectivity (%)												
Ethylene	98.3	83.1	51.5	36.4	30.5	89	97.1	83.0	55.1	44.9	48.8	77.0
Diethyl ether	0	0	0	0	0	0	2.9	0	0	0	0	0
Higher hydrocarbons												
C_{3-5}	0.2	3.6	5.7	6.5	8.5	5.3	0	5.7	10.4	8.7	8.4	11.8
C_6	0.5	4.3	4.8	5.2	8.8	2.7	0	3.3	4.6	4.4	7.1	5.9
C_7	1.0	2.6	3.0	5.7	12.2	1.8	0	3.5	3.9	4.5	3.9	1.6
C_8	0	3.2	5.8	9.2	8.6	1.2	0	2.7	4.8	4.7	5.8	1.3
C_{9+}	0	1.0	3.3	4.7	0.6	0	0	1.8	2.4	3.5	1.4	0.3
C_3–C_{9+} aliphatic (total)	1.7	14.7	22.6	31.3	38.7	11.0	0	17.0	26.1	25.8	26.6	20.9
C_6 (benzene)	0	1.8	0.7	0.8	0.4	0	0	0	0.6	0.4	0.2	0
C_7 (toluene)	0	0.4	1.4	2.4	2.6	0	0	0	1.6	2.7	2.1	0.5
C_8 (xylene)	0	0	3.8	7.4	7.2	0	0	0	4.1	8.9	10.7	0.9
C_9 (ethyl-methylbenzene)	0	0	12.6	11.0	11.4	0	0	0	8.3	10.6	8.5	0.4
C_9 (trimethylbenzene)	0	0	4.9	4.1	2.9	0	0	0	1.9	2.6	2.6	0.3
C_{9+}	0	0	2.5	6.6	6.3	0	0	0	2.3	4.1	0.5	0
C_6–C_{9+} aromatic (total)	0	2.2	25.9	32.3	30.8	0	0	0	18.8	29.3	24.6	2.1

Reaction conditions: 1.5 g catalyst; pure ethanol; 0.1 MPa; WHSV = 3.0 h^{-1}

Table 3 Product distribution at different temperatures over PZ-3.2 and PZ-3.4 catalysts

	PZ-3.2						PZ-3.4					
	Temperature (K)											
	553	573	613	653	673	713	553	573	613	653	673	713
Ethanol conversion (%)	78.4	98.8	100	100	100	100	52.3	97.9	100	100	100	100
Selectivity (%)												
Ethylene	60.6	99.0	97.0	76.6	71.9	98.7	58.7	99.8	99.7	99.4	99.6	99.8
Diethyl ether	39.4	1.0	0	0	0	0	41.3	0.2	0	0	0	0
Higher hydrocarbons												
$C_{3–5}$	0	0	2.1	9.5	10.6	0.3	0	0	0.3	0.6	0.4	0.2
C_6	0	0	0.9	4.5	7.7	1	0	0	0	0	0	0
C_7	0	0	0	4.4	3.3	0	0	0	0	0	0	0
C_8	0	0	0	3.0	3.7	0	0	0	0	0	0	0
C_{9+}	0	0	0	1.2	1.3	0	0	0	0	0	0	0
C_3–C_{9+} aliphatic (total)	0	0	3.0	22.6	26.6	1.3	0	0	0.3	0.6	0.4	0.2
C_6–C_{9+} aromatic (total)	0	0	0	0.8	1.5	0	0	0	0	0	0	0

Reaction conditions: 1.5 g catalyst; pure ethanol; 0.1 MPa; WHSV = 3.0 h^{-1}

Table 4 Product distribution at different temperatures over PZ-3.6 and PZ-5.1 catalysts

	PZ-3.6						PZ-5.1					
	Temperature (K)											
	553	573	613	653	673	713	553	573	613	653	673	713
Ethanol conversion (%)	43.4	40.0	100	100	100	100	11.6	23.0	27.3	49.3	100	100
Selectivity (%)												
Ethylene	23.0	57.1	96.2	98.8	99.6	99.3	3.2	4.2	16.1	78.6	99.4	99.6
Diethyl ether	77.0	42.9	0	0	0	0	96.8	95.8	83.9	21.4	0	0
Higher hydrocarbons												
C_3–C_{9+} aliphatic (total)	0	0	3.8	1.2	0.4	0.7	0	0	0	0	0.6	0.4
C_6–C_{9+} aromatic (total)	0	0	0	0	0	0	0	0	0	0	0	0

Reaction conditions: 1.5 g catalyst; pure ethanol; 0.1 MPa; WHSV = 3.0 h^{-1}

ethylene with a selectivity of 98.3% at 553 K. With increasing temperature, the ethylene selectivity decreases first due to the formation of higher hydrocarbons, passing through a minimum of nearly 30% at 673 K, and then increases again as a result of cracking reactions and coke rising. This result is corresponding to literature report [8, 9]. NH_3-TPD results (see Fig. 4a) show that parent HZSM-5 has the highest number of strong acid sites, which play a key role in the transformation of ethanol into hydrocarbons [7, 8, 28]. Therefore, a wide range of hydrocarbons are produced over HZSM-5 catalyst at high temperature.

Like in the case of parent HZSM-5 catalyst, the ethylene selectivity over PZ-1.9 catalyst (Table 2) decreases first, and then increases. However, the ethylene formation is enhanced at high temperatures (613–673 K). These observations may be rationalized as follows. The addition of P into HZSM-5 catalyst causes a sharp decrease of the strong acid (see Fig. 4b), thus would suppress the formation of higher hydrocarbons but enhance the production of ethylene [7, 14]. This can also be seen from the catalytic performance of PZ-3.2 catalyst (Table 3). Although the selectivity of ethylene is only 60.6% at 553 K, much lower than that over parent catalyst. The value increases greatly to 99.0% and 97.0% at the temperatures of 573 K and 613 K, respectively. Afterwards the formation of ethylene first decreases and then increases. As a result, ethylene is not the final product over PZ-1.9 and PZ-3.2 catalysts. Higher hydrocarbons are also observed at 653 K and 673 K.

An interesting finding is the production of ethylene over PZ-3.4 catalyst (Table 3). On this catalyst, the products are dominated by ethylene under all experimental conditions excepting the temperature of 553 K (diethyl ether is another

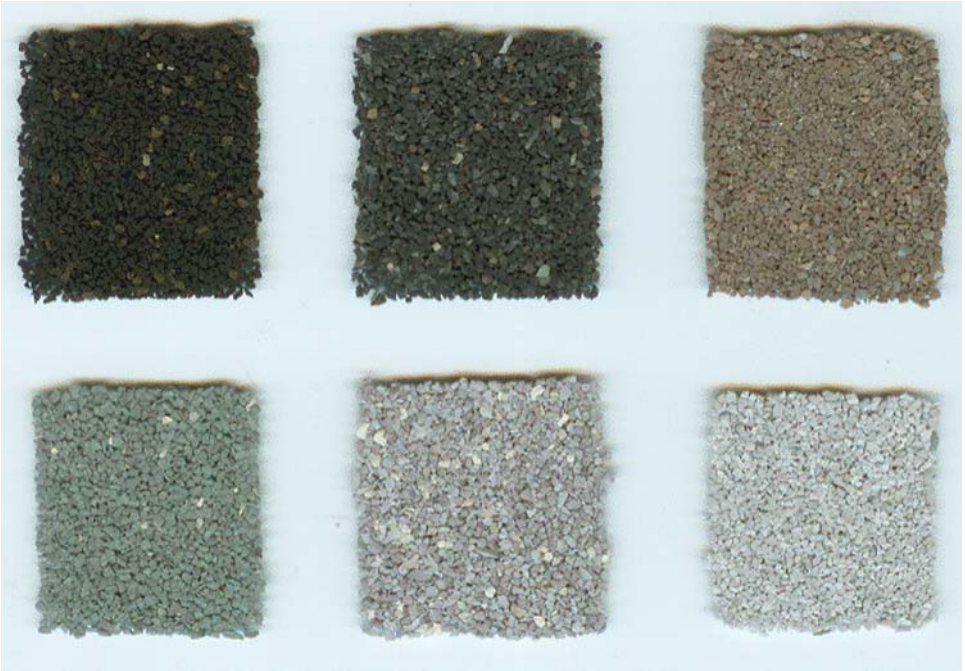

Fig. 5 Photographs of used catalysts. Upper graphs (from left to right): HZSM-5; PZ-1.9; PZ-3.2. Blow graphs (from left to right): PZ-3.4; PZ-3.6; PZ-5.1

product). The ethylene selectivity at 573–713 K is very high, not <99.4%, whereas those of higher hydrocarbons are relatively very low even at high temperatures. It indicates a high yield of ethylene in a broader range of temperatures over PZ-3.5 catalyst. The unique catalytic performance may be due to the presence of weak acid sites in this catalyst (see Fig. 4c). The weak acidic centers are unable to catalyze the formation of higher hydrocarbons [17]. Another factor may be the shape selective effect resulting from the decreased channel size of the catalyst (Fig. 2) [17, 29]. The higher hydrocarbons can hardly pass through the pores.

As for PZ-3.6 and PZ-5.1 catalysts (Table 4), higher reaction temperatures are necessary for dehydration of ethanol to ethylene. On PZ-3.6 catalyst, when the temperature is reached 613 K, the formation of ethylene becomes dominant. And over PZ-5.1 catalyst, the temperature should be above 673 K. When the reaction temperatures are below these temperatures (613 K, 673 K), diethyl ether occurs to a significant extent and ethylene is the final product for the sake of even weaker acidic centers left in these catalysts.

In addition, all of the used catalysts were collected and compared after reaction. More attractive results were obtained. Figure 5 is the photographs of the post-reaction catalysts. It can be observed that the color of the catalysts changes from black to gray with increasing P loading. Considering that coke deposition is usually a main reason for the deactivation of acidic catalyst [10, 13], the amount of carbonaceous deposits on these catalysts was measured by TG. As shown in Fig. 6, the weight loss of used HZSM-5 at 723–973 K, attributed to burning-off the coke, is about

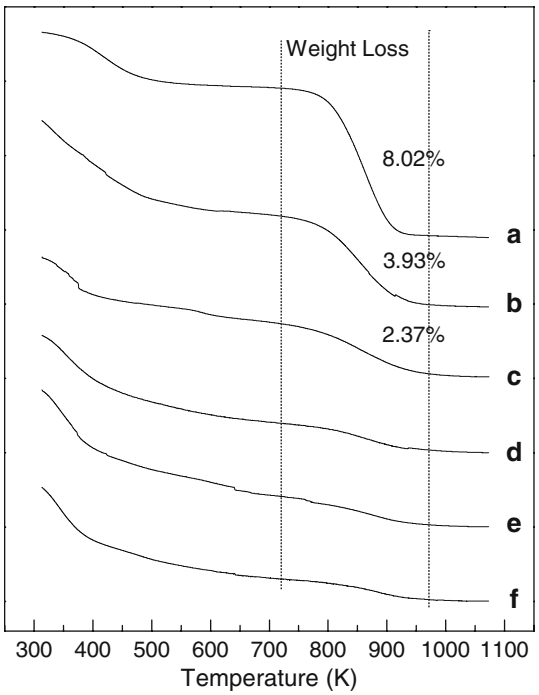

Fig. 6 TG curves of used catalysts: (**a**) HZSM-5; (**b**) PZ-1.9; (**c**) PZ-3.2; (**d**) PZ-3.4; (**e**) PZ-3.6; (**f**) PZ-5.1

8.02 wt%. For PZ-1.9 and PZ-3.2 samples, the weight loss decrease to 3.93 and 2.37 wt%, respectively. For the other catalysts, the values decrease to nearly 0.8 wt%. Combining this with the results of NH_3-TPD and the catalytic testing could indicate that P-modified HZSM-5 samples do

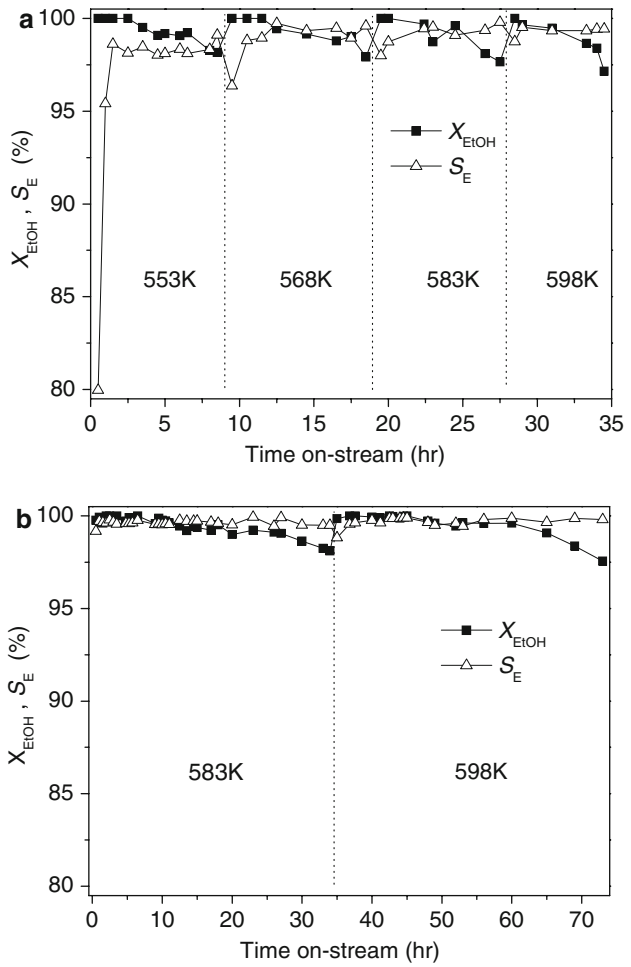

Fig. 7 The activity and stability of the catalysts: (**a**) HZSM-5; (**b**) PZ-3.4. Reaction conditions: 1.5 g catalyst; pure ethanol; 0.1 MPa; WHSV = 3.0 h^{-1}. X_{EtOH}: ethanol conversion; S_E: ethylene selectivity

not favor the bimolecular reactions involved in coke formation, and thus enhances the ability of anti-coking. Figure 7 gives a comparison of the stability by HZSM-5 and PZ-3.4 catalyst. The catalysts were deactivated gradually during the operation. So the reaction temperature was increased stepwise to maintain the X_{EtOH} above 98%. It can be seen that PZ-3.4 catalyst has a better stability than HZSM-5. From this point of view, the PZ-3.4 catalyst may be a better catalyst for catalytic dehydration of ethanol into ethylene because of the enhanced anti-coking ability and high selectivity of ethylene in a broader range of temperatures. Further work will continue to be done to understand the performance of this catalyst.

4 Conclusion

(1) Not all the P-modified HZSM-5 catalysts favor the reaction of dehydration of ethanol to ethylene at high temperature.

(2) When the P loading in the catalyst is low (1.9 and 3.2 wt%), the catalyst acidity decreases greatly due to dealumination of TFAL in the HZSM-5 framework. Ethylene is not the final product on these catalysts, and higher hydrocarbons are also detected at high temperatures.

(3) In the catalyst containing 3.4 wt% P (P/Al = 0.95), only weak acid sites are clearly observed. Over this catalyst, the main product is ethylene and the selectivity of ethylene is very high (≥99.4%) at the temperature range of 573–713 K.

(4) As the content of P is higher than 3.4 wt%, high reaction temperature is necessary for dehydration of ethanol to ethylene.

References

1. Zaki T (2005) J Colloid Interface Sci 284:606
2. Gucbilmez Y, Dogu T (2006) Ind Eng Chem Res 45:3496
3. Takahara I, Saito M, Matsuhashi H, Inaba M, Murata K (2007) Catal Lett 113:82
4. Varisli D, Dogu T, Dogu G (2007) Chem Eng Sci 62:5349
5. Chen GW, Li SL, Jiao FJ, Yuan Q (2007) Catal Today 125: 111
6. Le Van Mao R, Nguyen TM, Mclaughlin GP (1989) Appl Catal 48:265
7. Moser WR, Thompson RW, Chiang CC, Tong H (1989) J Catal 177:19
8. Chaudhuri SN, Halik C, Lercher JA (1990) J Mol Catal 62:289
9. Schulz J, Bandermann F (1994) Chem Eng Technol 17:179
10. Phillips CB, Datta R (1997) Ind Eng Chem Res 36:4466
11. Takahara I, Saito M, Inaba M, Murata K (2005) Catal Lett 105:249
12. Costa E, Uguina A, Aguado J, Hernandez PJ (1985) Ind Eng Chem Proc Des Dev 24:239
13. Aguayo AT, Gayubo AG, Atutxa A, Olazar M, Bilbao J (2002) Ind Eng Chem Res 41:4216
14. Le Van Mao R, Levesque P, Mclaughlin G, Dao LH (1987) Appl Catal 34:163
15. Jacobs JM, Jacobs PA and Uytterhoeven JB (1987) US Patent 4670620
16. Inaba M, Murata K, Saito M, Takahara I (2006) React Kinet Catal Lett 88:135
17. Tynjälä P, Pakkanen TT, Mustamäki S (1998) J Phys Chem B 102:5280
18. Scanlon JT, Willis DE (1985) J Chromatogr Sci 23:333
19. Poole CT (2003) The essence of chromatography, 2nd edn. Elseviser, Amsterdam
20. Zhuang JQ, Ma D, Yang G, Yan ZM, Liu XM, Liu XC, Han XW, Bao XH, Xie P, Liu ZM (2004) J Catal 228:234
21. Kaeding WW, Butter SA (1980) J Catal 61:155
22. Xue NH, Chen XK, Nie L, Guo XF, Ding WP, Chen Y, Gu M, Xie ZK (2007) J Catal 248:20
23. Caeiro G, Magnoux P, Lopes JM, Ramôa Ribeiro F, Menezes SMC, Costa AF, Cerqueira HS (2006) Appl Catal A: Gen 314:160
24. Zhao GL, Teng JW, Xie ZK, Jin WQ, Yang WM, Chen QL, Tang Y (2007) J Catal 248:29
25. Blasco T, Corma A, Martínez-Triguero J (2006) J Catal 237: 267

26. Cabral de Menezes SM, Lam YL, Damodaran K, Pruski M (2006) Microporous Mesoporous Mater 95:286
27. Tynjälä P, Pakkanen TT (1998) Microporous Mesoporous Mater 20:363
28. Széchényi A, Barthos R, Solymosi F (2006) Catal Lett 110:85
29. Damodaran K, Wiench JW, Cabral de Menezes SM, Lam YL, Trebosc J, Amoureux J-P, Pruski M (2006) Microporous Mesoporous Mater 95:296